

1 **Elaboration of a MALDI-TOF Mass Spectrometry-based Assay of Parkin Activity and**
2 **High-Throughput screening platform for Parkin Activators**

3 Ryan Traynor¹, Jennifer Moran¹, Michael Stevens¹, Axel Knebel¹, Bahareh Behrouz²,
4 Kalpana Merchant², C. James Hastie³, Paul Davies¹, Miratul M. K. Muqit¹ and Virginia De
5 Cesare¹

6 ¹ MRC Protein Phosphorylation and Ubiquitylation Unit, School of Life Sciences, University
7 of Dundee, Dow St, Dundee DD1 5EH, Scotland, UK

8 ²Vincere Biosciences Inc, 245 Main St. Fl 2, Cambridge, MA 02142, USA

9 ³ MRC Protein Phosphorylation and Ubiquitylation Unit Reagents and Services, School of
10 Life Sciences, University of Dundee, Dow St, Dundee DD1 5EH, Scotland, UK

11

12 **Abstract**

13 Parkinson's disease (PD) is a progressive neurological disorder that manifests clinically as
14 alterations in movement (bradykinesia, postural instability, loss of balance, and resting
15 tremors) as well as multiple non-motor symptoms including but not limited to cognitive and
16 autonomic abnormalities. Mitochondrial dysfunction has been linked to sporadic PD and loss-
17 of-function mutations in genes encoding the ubiquitin E3 ligase Parkin and protein kinase,
18 PTEN-induced kinase 1 (PINK1), that regulate mitophagy, are causal for familial and juvenile
19 PD¹⁻³. Among several therapeutic approaches being explored to treat or improve PD patient's
20 prognosis, the use of small molecules able to reinstate or boost Parkin activity represents a
21 potential pharmacological treatment strategy⁴. A major barrier is the lack of high throughput
22 platforms based on robust and accurate quantification of Parkin activity *in vitro*. Here we
23 present two different and complementary Matrix Assisted Laser Desorption/Ionization-Time of
24 Flight mass spectrometry (MALDI-TOF MS) based approaches for the quantification of Parkin
25 E3 ligase activity *in vitro*. These methods recapitulate distinct aspects of ubiquitin conjugation:
26 Parkin auto-ubiquitylation and Parkin-catalysed discharge on lysine residues. Both
27 approaches are scalable for high-throughput primary screening to facilitate the identification
28 of Parkin modulators.

29 **Introduction**

30 The coordinate action of the RING-IBR-RING (RBR) E3 ubiquitin ligase Parkin and PTEN-
31 induced kinase 1 (PINK1) is fundamental for the clearance of dysfunctional mitochondria by
32 mitophagy in nearly every cell type including neurons⁵⁻⁷. Under healthy cellular conditions,
33 Parkin is present in the cytosol in an auto-inhibited conformation⁸⁻¹⁰. Upon mitochondrial
34 depolarisation, that can be induced by mitochondrial uncouplers, PINK1 is activated and
35 recruits and activates Parkin at sites of mitochondrial damage via directly phosphorylating
36 Parkin at Serine 65 within its Ubiquitin-like domain (p-Parkin), and indirectly by
37 phosphorylating ubiquitin (p-Ub) also on Serine 65¹¹⁻¹³. Under *in vitro* assay conditions of
38 Parkin activation, Parkin and p-Parkin undergo auto-ubiquitylation on accessible lysine
39 residues; can catalyse ubiquitin transfer to substrates; or can stimulate discharge of ubiquitin
40 from charged E2 enzyme, UBE2L3, onto primary amines present in the reaction buffer
41 (discharge assay). Both types of ubiquitylation have previously been used as read-outs for
42 Parkin and p-Parkin activity determination¹³. Low-throughput, SDS page based-technique
43 have been extensively applied for visualizing Parkin autoubiquitylation patterns^{13,14}. Ubiquitin-
44 fluorescent probes have also been developed to exploit the reactivity of Parkin toward primary
45 amines¹⁵. While both these approaches have proved to be easy tools for investigating Parkin
46 activity *in vitro*, they have substantial caveats and limitations. SDS-page based techniques
47 lack scalability to high-throughput format and are often not fully quantitative while fluorescent
48 based-approaches are intrinsically prone to fluorescence related artefacts. Herein we have
49 elaborated two quantitative and complementary Matrix Assisted Laser Desorption/Ionization-
50 Time of Flight mass spectrometry (MALDI-TOF MS) based assays to determine Parkin and
51 p-Parkin activity *in vitro*. Both methods allow for quantitative investigation of Parkin activity *in*
52 *vitro*; are scalable to high-throughput formats and employ physiological substrates (ubiquitin
53 and p-ubiquitin) thus circumventing artefacts associated with the use of fluorescence-based
54 tools.

55 **Results**

56 **Development of MALDI-TOF Parkin Activity assays**

57 We previously reported the development of a MALDI-TOF MS based method for the
58 quantification of the activity of ubiquitin E2 conjugating enzymes and E3 ligases belonging the
59 RING, HECT and RBR family¹⁶. While RING E3 ligases rely on the catalytic activity of a
60 cognate E2 conjugating enzyme, HECT and RBR E3 ligases receive ubiquitin from the E2
61 conjugating enzymes to ubiquitylate their substrate on lysine residues. Most E3 ligases will
62 undergo autoubiquitylation when tested *in vitro*. The previously published MALDI-TOF E2/E3

63 assay was based on quantification of the progressive disappearance of ubiquitin as a
64 consequence of its utilisation in the auto-ubiquitylation process¹⁶. Since the reactivity towards
65 lysine is mediated by the E3 ligase in the RBR enzymatic cascade, we explored whether we
66 could determine Parkin reactivity using a complementary lysine discharge method (also
67 known as nucleophile reactivity assay¹⁷) of untagged (His-SUMO cleaved) recombinant
68 human Parkin expressed in *E.coli* as previously described¹⁸. UBE2L3 is a HECT-RBR specific
69 E2 conjugating enzyme that lacks intrinsic E3-independent reactivity towards lysine
70 residues¹⁷. Therefore, the ability to discharge on lysine – and the consequent formation of
71 ubiquitin-lysine adducts (Ub-K) - relies exclusively on the activity of a cognate HECT or RBR
72 E3 ligase. In the auto-ubiquitylation assay, quantification of Parkin activity is achieved by
73 comparing the signal of ubiquitin to that of the heavy-labelled ubiquitin internal standard (¹⁵N-
74 Ub). Therefore, the autoubiquitylation rate can be represented as a linear reduction of
75 detectable ubiquitin over time (Residual Ubiquitin %) (Fig. 1A). In contrast, in the discharge
76 assay, both substrate (Ub) and product (Ub-K) change over time as the former is converted
77 to the latter. Consequently, the mathematical representation of the discharge assay method
78 will be a non-linear function, as both substrate and product measurements change over time
79 (Fig. 1B). Therefore, in the discharge assay, a dedicated standard curve must be defined in
80 advance to determine the rate of product formation (Ub-K Formation %) (Fig. 1B and Sup Fig
81 5). The unique regulation of WT Parkin requires the combined use of ubiquitin and
82 phosphorylated ubiquitin (p-Ub). The interaction between p-Ub and Parkin releases Parkin's
83 autoinhibitory state, therefore p-Ub functions as an allosteric Parkin modulator. Due to the
84 closeness in molecular weight between p-Ub (8646.7 *m/z*) and the ¹⁵N ubiquitin internal
85 standard (8669.7 *m/z* observed), we employed His₆-tagged-p-Ub (p-Ub-His, 9812 *m/z*, See
86 Sup. Fig 1) to prevent interference with the ¹⁵N ubiquitin signal. The His₆ tag present at the C-
87 terminus of p-Ub-His and the absence of a final glycine dyad (See Sup Fig. 1) do not allow for
88 the incorporation of p-Ub-His into poly-ubiquitin chains, although lysine available in the p-Ub-
89 His may still be employed as ubiquitin substrate. The autoubiquitylation assay exhibited
90 slower kinetics compared to the discharge assay and therefore, to achieve comparable
91 reaction rates, the autoubiquitylation assay was performed at 37 °C while the discharge assay
92 was performed at room temperature. Due to the difference in the experimental settings, the
93 results obtained from the two assays cannot be directly compared, although they aligned each
94 other very closely.

95 **Assessing Parkin activity by MALDI-TOF MS autoubiquitylation and discharge assay**

96 The activity of Parkin is tightly regulated both by direct phosphorylation and by the interaction
97 with phosphorylated ubiquitin^{6,13}. We employed the MALDI-TOF autoubiquitylation and
98 discharge assays to accurately quantify the contribution of these regulatory layers on Parkin
99 activity rate. In the autoubiquitylation assay, Parkin activity was quantified by the progressive
100 reduction of the mono-ubiquitin peak (Fig. 1A) while in the discharge assay Parkin activity was
101 assessed by the formation of Ub-Ac-K product (Fig. 2A). Both MALDI-TOF MS methods were
102 employed to quantify the increment in recombinant Parkin and p-Parkin (expressed as
103 previously described¹⁸, Sup. Fig 3A-B) activity rates upon addition of p-Ub-His. WT Parkin and
104 p-Parkin were tested at a final concentration of 500 nM. Reactions were started by the addition
105 of ubiquitin supplemented with three different concentrations of p-Ubi: 100 nM, 500 nM and
106 2500 nM. In the autoubiquitylation assay, data were firstly normalized over the ¹⁵N Ubiquitin
107 internal standard signal (Light Ub/¹⁵N Ub) and a control reaction without Parkin present
108 (E1+E2 control) was used to establish the rate of Parkin-dependent ubiquitin consumption
109 (Sup. Fig1A and B). We found that an amount of p-Ub-His stoichiometrically equivalent to WT
110 Parkin (500 nM) is sufficient to partially activate WT Parkin (Fig. 2A), while 5 times excess of
111 p-Ub-His induced WT Parkin activity levels comparable to those of p-Parkin in absence of p-
112 Ub-His (Fig. 2A). Stoichiometric amounts of p-Ub-His double the autoubiquitylation rate of p-
113 Parkin after 10 minutes (Residual Ubiquitin 66% in absence of p-Ub compared to 31.5% in
114 presence of 500 nM p-Ub). In the discharge assay, WT Parkin is efficiently activated by
115 stoichiometric amounts of p-Ub-His. A similar effect was observed for p-Parkin, whose activity
116 is greatly enhanced already in presence of sub-stoichiometric amounts of p-Ub-His (Ub-K
117 Formation 22 % in absence of p-Ub compared to 78% in presence of 100 nM p-Ub) (Figure
118 2B). Phos-tag SDS-gel analysis indicated that about 80% of Parkin was phosphorylated (Sup
119 Fig. 3), therefore, when testing p-Parkin in presence of p-Ub-His, it is not possible to
120 discriminate whether the increase in activity is due to the activation of WT Parkin compared
121 to overactivation of p-Parkin. Overall, both MALDI-TOF based assays accurately and
122 quantitatively measured the E3 ligase activity of Parkin and p-Parkin and the rate at which the
123 co-factor p-Ub-His activates WT Parkin and may further activate p-Parkin.

124 **Quantifying the effect of point mutations on Parkin activity**

125 Structural analysis of inactive and active Parkin has identified three major inter-domain
126 interfaces that that maintain auto-inhibition of Parkin Ub ligase activity^{9,10,19}. Based on these
127 studies, engineering point mutations that disrupt the repressor element of Parkin (REP)
128 domain interaction with the RING1 (really interesting new gene 1) domain-interface, W403A,

129 or the RING0-RING2 interface, F146A and F463Y, that each loosen the auto-inhibitory
130 conformation of Parkin and are effective at releasing Parkin activity^{9,10,20,21} as well as rescuing
131 defects in p-Ub binding and Ser65 phosphorylation²¹. We therefore expressed Parkin W403A,
132 F463Y and F146A mutants as well as the catalytic inactive C431A mutant (Sup. Fig. 3C) and
133 compared the impact of these mutations on Parkin activation using both the Parkin
134 autoubiquitylation and discharge MALDI-TOF MS based assays. Since these Parkin
135 activating-mutants only partially release E3 ligase activity, enzymatic concentrations and
136 incubation times were optimized and we consequently observed activity levels lower than
137 activated WT Parkin or p-Parkin. The activity of W403A Parkin could not be detected in
138 absence of p-Ub-His at the concentration of 500 nM (Sup Fig.3) while it was detected at the
139 final concentration of 2 μ M (Fig. 3A). The lack of W403A activity at low concentration (500
140 nM) and in absence of the co-factor p-Ub-His is due to the relatively low level of activity
141 released by this point mutation. Therefore W403A, F146A and F463Y mutants were tested at
142 the final concentration of 2 μ M and incubation time extended up to 120 minutes. W403A
143 background autoubiquitylation activity (in absence of p-Ub-His) halves the initial ubiquitin pool
144 in about 90 minutes of incubation (Fig. 3A) and down to a 32.3% of the total at the final time
145 point of 120 minutes. Further activation is achieved in presence of increasing amounts of p-
146 Ub-His (Fig. 3A). The F146A mutant showed a level of activity comparable to those of W403A,
147 with only 36.2% of the initial pool of ubiquitin still detectable after 120 minutes. The active
148 mutant F463Y was about 50% less active compared to W403A and F146A mutants (66.7%
149 of ubiquitin still present after 120 minutes). A similar trend was observed in the discharge
150 assay, albeit the measured activity of the mutants in the discharge assay were relatively low
151 that likely reflects the distinct temperature at which respective assays were performed. We
152 confirmed these findings using an orthogonal Parkin *in vitro* assay in which mutant Parkin
153 F463Y, F164A and W403A and C431F were incubated in the presence of adenosine
154 triphosphate (ATP), MgCl₂, E1 ubiquitin-activating ligase, UbCH7 conjugating E2 ligase and
155 ubiquitin. After 60 minutes, reactions were terminated with SDS sample buffer in the presence
156 of 2-mercaptoethanol and heated at 100 °C, and ubiquitylation was assessed by immunoblot
157 analysis with antibodies that detect ubiquitin (Fig 3C). We further employed the MALDI-TOF
158 based assays to estimate the half maximal effective concentration (EC₅₀) of p-Ub-His for the
159 activation of WT, W403A and F126A Parkin. We incubated 500 nM WT, W430A and F146A
160 Parkin with increasing concentrations of p-Ub-His (0.05 μ M, 0.2 μ M, 0.5 μ M, 1 μ M, 2.5 μ M
161 and 5 μ M) and incubated the reaction 30 minutes in the previously defined conditions. An
162 estimated EC₅₀ of 2 μ M for WT Parkin, 0.2 μ M for W403A and 0.4 μ M for F146A was

163 determined in the MALDI-TOF autoubiquitylation assay settings. Similar trend was observed
164 for the MALDI-TOF discharge assay: 1.4 μM for WT Parkin, 0.5 μM for W403A and 0.6 μM
165 for F146A. The results confirmed that both W403A and F146A Parkin mutants require reduced
166 amount of p-Ub-His to achieve activity levels comparable to those of WT Parkin. Both assays
167 indicates that the W403A mutation requires between 2 and 10 less p-Ub-His to achieve WT
168 Parkin activity levels. Overall, our analysis of Parkin mutants is consistent with the previous
169 literature reporting W403A as one of the most activating Parkin single point mutations^{9,10,19}.
170 Moreover, the accurate quantification of the absolute and relative activation effect of Parkin
171 point mutations further validates the ability of both MALDI-TOF based assays to identify Parkin
172 activation and inhibition rates.

173

174 **Development of Parkin High-Throughput Screen (HTS)**

175 Primary, activity based high-throughput screening (HTS) represents often the first step when
176 starting a new drug discovery project that targets an enzyme. Such a step is fundamental for
177 the identification of promising candidates from the vast number of natural and synthetic
178 compound libraries available. Since PD is caused by loss of function of Parkin, the
179 pharmaceutical intent is to re-instate the enzymatic activity of Parkin through the identification
180 of Parkin-specific activators. The Parkin auto-ubiquitylation assay relies on the progressive
181 reduction of the ubiquitin signal. In such conditions, the identification of activators will be
182 limited by the assay window itself. On the other hand, the discharge assay offers a larger
183 assay window and the possibility to work at lower temperature (25°C). Therefore, we tested
184 the feasibility of employing the MALDI-TOF based discharge assay to perform a preliminary
185 high-throughput screen for the identification of p-Parkin activators. We tested a compound
186 library of about 20000 compounds predicted to be able to permeate the blood brain barrier.
187 The HTS workflow was designed to be scalable and adaptable for a high-throughput screening
188 campaign and consists of 3 steps: pre-incubation of 5 μL enzymatic mixture with compounds
189 (10 μM in 100% DMSO), reaction initiation by adding 5 μL of substrate (mono-ubiquitin and
190 50 mM Ac-K) and reaction termination with 5 μL 6% TFA (Fig 4A). A total of 60 x 384 well
191 plates were divided into nine smaller batches of up to 8 x 384 well plates (about 2800
192 compounds) to be processed daily (Fig. 4 D and E). The use of high-density 1536 AnchorChip
193 MALDI targets allowed to combine up to four 384 assay plates into one MALDI-TOF MS run
194 (Fig 4A). Each plate included a column (16 wells) reserved for positive controls (no compound
195 present, only DMSO) and one column for negative controls (reaction in absence of p-Parkin

196 where only background reading should be detected, example data in Fig. 4B). Data were
197 normalized by dividing the area of the substrate (Ub) to the area of the product (Ub-Ac-K). A
198 linearity curve with known amounts of Ub and Ub-Ac-K was interpolated and used to translate
199 Ub-Ac-K /Ub ratio into % of Ub-K formation (Sup. Fig 5). The robustness of HTS screening is
200 a function of both the variability of positive and negative controls and the statistical space for
201 the robust identification of the compound related effect. A Z' Prime value > 0.5 is considered
202 a robust assay. The Z' Prime average for the MALDI-TOF discharge assay was 0.75 with only
203 one 384 plate scoring below the threshold of 0.5 (Fig. 4C) confirming the robustness of the
204 assay and the employability in HTS campaigns. An arbitrary and stringent hit cut-off of +/-
205 25% activity compared to the control was applied to select compounds to be further
206 investigated. A total of 5 compounds reduced p-Parkin activity by more than 25% and only 1
207 compound scored as potential activator for a total of 6 positive hits. Given the low number of
208 compounds tested, it was not unexpected that none of the positive hits were confirmed by
209 subsequent validation analysis by IC50 calculation. Identification of genuine active
210 compounds, inhibitors and particularly activators, are a few and far in between, however the
211 HTS screening results indicated an exceptionally low false positive rate (FPR) of 0.028%
212 confirming the advantages of MALDI-TOF based read-out compared to fluorescence-based
213 approaches. Several activators of Parkin have been described in patent literature, although
214 peer-reviewed research is not available. We tested three molecules reported in patent WO
215 2018/023029 (chemotype B1, B2 and C1, Sup. Fig. 6A) for their ability to activate Parkin. All
216 compounds were tested at a final concentration of 50 μ M in a time course experiment (7 time
217 points) against WT-Parkin (activated by equimolar amounts of p-Ub-His) and p-Parkin using
218 both the MALDI-TOF autoubiquitylation assay (Sup Fig. 6B) and the discharge assay (Sup.
219 Fig. 6C). The MALDI-TOF autoubiquitylation assay did not detect a statistically significant
220 differences between the control (DMSO only) and the tested compounds against either WT
221 Parkin or p-Parkin (Sup. Fig. 6B). However, the MALDI-TOF discharge assay successfully
222 detected a small but statistically significant activation effect on WT-Parkin in presence of
223 chemotype B2 after 50 and 60 minutes of incubation while no effect was observed against p-
224 Parkin. These results indicate that the MALDI-TOF discharge assay might prove more
225 sensitive for the detection of small changes in enzymatic activity compared to the auto-
226 ubiquitylation assay. This can be explained by the relatively easy access of Ac-Lysine to the
227 Parkin active site already in presence of weak structural perturbations. Overall, our results
228 confirmed the ability of the previously reported chemotype B2 to enhance WT-Parkin and
229 validated the ability of the MALDI-TOF discharge assay to effectively detect Parkin activators.

230 Discussion

231 Accumulating of biological and structural studies have provided unprecedented understanding
232 of the regulation of Parkin by either direct phosphorylation on serine 65 or by the interaction
233 with phosphorylated ubiquitin. Currently, the *in vitro* quantification of Parkin's activity relies on
234 the use of SDS-PAGE followed by antibody-based detection of ubiquitylation events. This
235 method enables assessment of Parkin's activity via monitoring Parkin auto-ubiquitylation
236 pattern; multi-monoubiquitylation of substrates such as MIRO1²², mono-ubiquitylation of
237 UBE2L3^{10,12} or the formation of free ubiquitin chains^{10,23,1}. Such approaches are intrinsically
238 low throughput and time consuming. Here we reported two robust MALDI-TOF based assays
239 to investigate the activity of Parkin in a fast, quantitative and high-throughput fashion. Both
240 MALDI-TOF based assays accurately and quantitatively recapitulate Parkin activity and
241 activation rates in presence of the activating cofactor p-Ub-His. Structural studies have
242 revealed point mutations known to partially release Parkin auto-inhibitory state and release
243 background activity. The MALDI-TOF based technology enabled facile comparison and
244 quantification of the relative impact of such point mutations on Parkin activity. Whilst this assay
245 will aid in understanding the regulation of Parkin activity by academic researchers, MALDI-
246 TOF based technologies are emerging as the gold standard in the drug discovery space.
247 Fluorescence probes as UbMes and UbFluor have been reported as functional Ub-based
248 probes for determining Parkin activity¹⁵. Such strategies are potentially scalable to high-
249 throughput screening levels; however, the use of fluorescence as analytical read-out is
250 inherently problematic because of fluorescence artefacts that result in both false positives and
251 false negatives. For example, UbFluor is labile in the presence of reducing agents or other
252 small molecules that possess thiol or amine groups that may cleave UbFluor even in the
253 absence of RBR E3, resulting in false positives¹⁴. Fluorescent small molecules may also
254 disrupt fluorescence polarization readings, resulting in false negatives. Rate of false positive
255 and negative is highly dependent on the fluorophore used, the stability of the substrate, the
256 assay conditions and the nature of the chemical libraries tested. A recent study suggested
257 that false discovery rate might score anywhere between 0.5 to 9.9% depending on the assay
258 and type of fluorescence used²⁴. This translates into the risk of following up on false leads,
259 with obvious consequences in terms of increased costs and reduced efficiency. The screening
260 of ~20000 compounds by MALDI-TOF MS discharge assay resulted in a false positive rate of
261 only 0.028%, well below what to be expected with fluorescent based tools.

262 The social and economic impact of PD has sustained intense research efforts to identify
263 pharmacological treatments, producing several patents reporting chemical structures of
264 Parkin activators. Here we tested three previously reported molecules using both the MALDI-
265 TOF MS auto-ubiquitylation and discharge assay. Our results confirmed the expected Parkin-
266 activation effect of one of these molecules by the MALDI-TOF discharge assay while no
267 activation effect was observed by the MALDI-TOF auto-ubiquitylation assay. Notably, the HTS
268 MALDI-TOF base strategy can also be easily applied to other RBR E3 ligases (as has been
269 done for HOIP¹⁶) including those E3 ligases that peculiarly discharge on non-canonical
270 residues (for example serine and sugars) such as HOIL-1 and RNF213^{25,26}. Overall, we
271 anticipate MALDI-TOF based technologies to substantially increase our understanding of the
272 functioning of E2 conjugating enzymes and E3 ligases by providing accurate and quantitative
273 data and to contribute to drug discovery campaigns in the ubiquitin field.

274

275 **Materials & Methods**

276 **Reagents**

277 Ubiquitin was acquired by sigma Aldrich (U6253). Eppendorf Low-Bind 384 well plates (Cat.
278 Number 951031305) were used for low-throughput assay. Ac-K was purchased from
279 Bachem/Cambridge (Cat. Number 4000486.0001). p-Ub-His, ¹⁵N Ubiquitin, Ube1, Ube2L3,
280 WT and phosphorylated Parkin and Parkin point mutants were expressed and purified in
281 house as indicated in below.

282 **Autoubiquitylation MALDI-TOF MS Parkin Activity assay**

283 200 nM E1 activating enzyme, 1000 nM UBE2L3 conjugating enzyme, 1000 nM WT parkin or
284 p-Parkin, 20 mM MgCl₂, 2 mM ATP, 0.05% BSA and 2 mM TCEP were mixed in 1X phosphate
285 buffer (PBS, pH 8.5) and aliquoted into Eppendorf Low-Bind plates (5 µL per well). The
286 reactions were started by adding 5 µL of 50 µM Ubiquitin (in 1X PBS, pH 8.5) supplemented
287 with the indicated amount of p-Ub-His. Plates were sealed with adhesive aluminium foil and
288 incubated at 37°C in an Eppendorf ThermoMixer C (Eppendorf) equipped with a ThermoTop
289 and a SmartBlock™ PCR 384. The reactions were stopped at the indicated time points by the
290 addition of 5 µL 6% TFA supplemented with 6 µM ¹⁵N Ubiquitin. Samples were spotted on
291 1536 AnchorChip MALDI target using a Mosquito nanoliter pipetting system (TTP Labtech)
292 and analysed by MALDI-TOF MS as previously reported¹⁶.

293 **Discharge MALDI-TOF MS Parkin Activity assay**

294 An identical enzymatic mixture as the autoubiquitylation assay was prepared. The reactions
295 were started by adding 5 μ L of 50 μ M Ubiquitin supplemented with the indicated amount of p-
296 Ub-His and 50 mM Ac-K. Plates were incubated at room temperature (25 degrees) and sealed
297 with adhesive aluminium foil. The reactions were stopped at the indicated time points by the
298 addition of 5 μ L 6% TFA.

299 **Parkin HTS screening**

300 All Parkin HTS assays were performed in a total volume of 20.01 μ l at room temp using a
301 FluidX Xrd-384 dispenser. To plates containing 20nl of compound 10ul of a mix containing
302 500nM p-PARKIN, 400nM UBE1, 4000nM UBE2L3, 20 μ M MgCl₂, 2mM ATP in a 50mM
303 HEPES pH8.5 20mM TECEP buffer was added. The plates were preincubated at 25°C for
304 30mins and the assay was then initiated with the addition of 10 μ L of Ubiquitin mix containing
305 100 μ M Ubiquitin, 100mM Ac-lysine. The assay was incubated for 20mins at 25°C. The assay
306 was then terminated with the addition of 10 μ l 6% TFA.

307 **Expression and Purification of recombinant GST-PINK1 126-end (pediculus humanus).**

308 BL21 codon plus cells were transformed with MRC-PPU plasmid DU34798. A single antibiotic
309 resistant colony was selected and propagated for 16 h at 37°C, 200 rpm. 12 x 1L batches of
310 LB broth/carbenicillin were inoculated with the overnight culture and grown until an OD₆₀₀ of
311 0.8. The incubation temperature was dropped to 26°C and PINK1 expression was induced by
312 supplementing the media with 0.1 mM Isopropyl β -D-1-thiogalactopyranoside (IPTG) and left
313 to express for overnight. The cells were collected by centrifugation (25 min at 4200 rpm) and
314 the clarified broth was decanted. The cells were resuspended in 20 ml per pellet of 50 mM
315 Tris pH 7.5, 250 mM NaCl, 1 mM DTT, 1 mM AEBSF, 10 μ g/ml Leupeptin. The suspension
316 was collected into 50 ml centrifuge vials, chilled on ice and sonicated using 6 pulses of 55%
317 amplitude and 15 s pulses. The suspension was clarified by centrifugation at 40000 x g for
318 25 min at 4°C. 6 ml GSH-agarose was equilibrated with wash buffer (50 mM Tris pH 7.5,
319 250 mM NaCl, 1 mM DTT) and mixed with the clarified cell lysate for 90 min. The GSH-
320 agarose was recovered by sedimentation, washed 5 times with 5 volumes of wash buffer and
321 eluted in wash buffer containing 10 mM reduced GSH.

322 **Expression and Purification of recombinant Parkin 1-465 (human), Parkin active**
323 **mutants and p-Parkin.**

324 Human wild type Parkin 1-465 along with the F146A, W403A, and F463Y mutants (MRC-PPU
325 plasmids DU40847, DU44642, DU44643 and DU58844) were expressed as His6-SUMO-
326 fusion proteins and purified as described previously¹²

327 To produce phosphorylated Parkin, the fusion protein was captured on Ni-agarose, washed
328 and incubated with 5 mg of GST-PINK1 126-end in the presence of 10 mM MgCl₂ and 2 mM
329 ATP for 4 h at 27°C. The initial kinase and Mg-ATP were removed and replaced with fresh
330 kinase and Mg-ATP for incubation over night at 27°C. The Ni-agarose was washed three times
331 with wash buffer and Parkin was eluted in the smallest possible volume. The protein was then
332 dialysed in the presence of SENP1 as previously described^{12,13} The protein was further
333 phosphorylated with more PINK1 and Mg-ATP and at the same time concentrated to 6 mg/ml.
334 Finally, the protein was purified further by chromatography on a Superdex 200 as described
335 above and concentrated to about 2 mg /ml. Note that phosphorylated Parkin is more soluble
336 than unphosphorylated Parkin and yields are generally higher.

337

338 **Expression and Purification of recombinant p-Ubiquitin-His (pSer65-Ubiquitin-6His),** 339 **¹⁵N Ubiquitin and Ub-K**

340 Ubiquitin-His₆ was produced from a kanamycin resistance conferring plasmid MRC-PPU
341 reagent DU21990. The cells were grown and induced as for untagged ubiquitin, but they were
342 collected and lysed in 50 mM Tris pH 7.5, 250 mM NaCl, 25 mM imidazole, 7 mM 2-
343 mercaptoethanol, 10 µg/ml Leupeptin (Apollo Scientific), 1 mM AEBSF (Apollo Scientific). The
344 protein was purified over Ni-NTA agarose, eluted into a 0.4 M imidazole buffer and dialysed
345 against 50 mM Tris pH 7.5, 200 mM Tris pH 7.5, 7 mM 2-mercapto ethanol. For
346 phosphorylation at Ser65, 20 mg of Ubiquitin-His was incubated with 2 mg of GST-PINK1 in
347 the presence of 10 mM MgCl₂ and 2 mM ATP for overnight at 28°C. The Ubiquitin-His was
348 collected on 1 ml Ni-NTA agarose, washed 4 times with 12 bed volumes of 50 mM Tris pH
349 7.5, 200 mM Tris pH 7.5, 7 mM 2-mercapto ethanol and recovered by elution with imidazole.
350 Imidazole was removed and p-Ub-His concentrated using Millipore Ultra filter (3000 MWCO)
351 followed by subsequent sample dilution in 1x PBS, pH 7.0. The sequence was repeat for 6
352 times using a 6-fold dilution. Phosphorylation efficiency was assessed by LC-MS analysis
353 (Sup. Fig 1): 70% of Ub-His was successfully phosphorylated. No further purification step was
354 performed, the relative purity was considered in the experimental calculations. Expression
355 and purification of ¹⁵N-Ubiquitin and Ub-K was performed as previously reported^{27,28}.

356

357

358 M.M.K.M. is supported by a Wellcome Trust Senior Research Fellowship in Clinical Science
359 (210753/Z/18/Z); the Michael J Fox Foundation; and an EMBO YIP Award.

360

361 **References**

- 362 1 Corti, O., Lesage, S. & Brice, A. What genetics tells us about the causes and mechanisms of
363 Parkinson's disease. *Physiol Rev* **91**, 1161-1218, doi:10.1152/physrev.00022.2010 (2011).
- 364 2 Kitada, T. *et al.* Mutations in the parkin gene cause autosomal recessive juvenile parkinsonism.
365 *Nature* **392**, 605-608, doi:10.1038/33416 (1998).
- 366 3 Valente, E. M. *et al.* Hereditary early-onset Parkinson's disease caused by mutations in PINK1.
367 *Science* **304**, 1158-1160, doi:10.1126/science.1096284 (2004).
- 368 4 Miller, S. & Muqit, M. M. K. Therapeutic approaches to enhance PINK1/Parkin mediated
369 mitophagy for the treatment of Parkinson's disease. *Neurosci Lett* **705**, 7-13,
370 doi:10.1016/j.neulet.2019.04.029 (2019).
- 371 5 Narendra, D. P. & Youle, R. J. Targeting mitochondrial dysfunction: role for PINK1 and Parkin in
372 mitochondrial quality control. *Antioxid Redox Signal* **14**, 1929-1938, doi:10.1089/ars.2010.3799
373 (2011).
- 374 6 Koyano, F. *et al.* Ubiquitin is phosphorylated by PINK1 to activate parkin. *Nature* **510**, 162-166,
375 doi:10.1038/nature13392 (2014).
- 376 7 Shiba-Fukushima, K. *et al.* PINK1-mediated phosphorylation of the Parkin ubiquitin-like domain
377 primes mitochondrial translocation of Parkin and regulates mitophagy. *Sci Rep* **2**, 1002,
378 doi:10.1038/srep01002 (2012).
- 379 8 Chaugule, V. K. *et al.* Autoregulation of Parkin activity through its ubiquitin-like domain. *EMBO J*
380 **30**, 2853-2867, doi:10.1038/emboj.2011.204 (2011).
- 381 9 Kumar, A. *et al.* Disruption of the autoinhibited state primes the E3 ligase parkin for activation and
382 catalysis. *EMBO J* **34**, 2506-2521, doi:10.15252/embj.201592337 (2015).
- 383 10 Trempe, J. F. *et al.* Structure of parkin reveals mechanisms for ubiquitin ligase activation. *Science*
384 **340**, 1451-1455, doi:10.1126/science.1237908 (2013).
- 385 11 Sauve, V. *et al.* A Ubl/ubiquitin switch in the activation of Parkin. *EMBO J* **34**, 2492-2505,
386 doi:10.15252/embj.201592237 (2015).
- 387 12 Kondapalli, C. *et al.* PINK1 is activated by mitochondrial membrane potential depolarization and
388 stimulates Parkin E3 ligase activity by phosphorylating Serine 65. *Open Biol* **2**, 120080,
389 doi:10.1098/rsob.120080 (2012).
- 390 13 Kazlauskaitė, A. *et al.* Parkin is activated by PINK1-dependent phosphorylation of ubiquitin at
391 Ser65. *Biochem J* **460**, 127-139, doi:10.1042/BJ20140334 (2014).
- 392 14 Foote, P. K. & Statsyuk, A. V. Monitoring PARKIN RBR Ubiquitin Ligase Activation States with
393 UbFluor. *Curr Protoc Chem Biol* **10**, e45, doi:10.1002/cpch.45 (2018).
- 394 15 Park, S., Foote, P. K., Krist, D. T., Rice, S. E. & Statsyuk, A. V. UbMES and UbFluor: Novel probes for
395 ring-between-ring (RBR) E3 ubiquitin ligase PARKIN. *J Biol Chem* **292**, 16539-16553,
396 doi:10.1074/jbc.M116.773200 (2017).

- 397 16 De Cesare, V. *et al.* The MALDI-TOF E2/E3 Ligase Assay as Universal Tool for Drug Discovery in the
398 Ubiquitin Pathway. *Cell Chem Biol* **25**, 1117-1127 e1114, doi:10.1016/j.chembiol.2018.06.004
399 (2018).
- 400 17 Wenzel, D. M., Lissounov, A., Brzovic, P. S. & Klevit, R. E. UBC7 reactivity profile reveals parkin
401 and HHARI to be RING/HECT hybrids. *Nature* **474**, 105-108, doi:10.1038/nature09966 (2011).
- 402 18 Kazlauskaitė, A. *et al.* Binding to serine 65-phosphorylated ubiquitin primes Parkin for optimal
403 PINK1-dependent phosphorylation and activation. *EMBO Rep* **16**, 939-954,
404 doi:10.15252/embr.201540352 (2015).
- 405 19 Wauer, T. & Komander, D. Structure of the human Parkin ligase domain in an autoinhibited state.
406 *EMBO J* **32**, 2099-2112, doi:10.1038/emboj.2013.125 (2013).
- 407 20 Riley, B. E. *et al.* Structure and function of Parkin E3 ubiquitin ligase reveals aspects of RING and
408 HECT ligases. *Nat Commun* **4**, 1982, doi:10.1038/ncomms2982 (2013).
- 409 21 Tang, M. Y. *et al.* Structure-guided mutagenesis reveals a hierarchical mechanism of Parkin
410 activation. *Nat Commun* **8**, 14697, doi:10.1038/ncomms14697 (2017).
- 411 22 Kazlauskaitė, A. *et al.* Phosphorylation of Parkin at Serine65 is essential for activation: elaboration
412 of a Miro1 substrate-based assay of Parkin E3 ligase activity. *Open Biol* **4**, 130213,
413 doi:10.1098/rsob.130213 (2014).
- 414 23 Antico, O. *et al.* Global ubiquitylation analysis of mitochondria in primary neurons identifies
415 endogenous Parkin targets following activation of PINK1. *Sci Adv* **7**, eabj0722,
416 doi:10.1126/sciadv.abj0722 (2021).
- 417 24 Borrel, A. *et al.* High-Throughput Screening to Predict Chemical-Assay Interference. *Sci Rep* **10**,
418 3986, doi:10.1038/s41598-020-60747-3 (2020).
- 419 25 Kelsall, I. R., Zhang, J., Knebel, A., Arthur, J. S. C. & Cohen, P. The E3 ligase HOIL-1 catalyses ester
420 bond formation between ubiquitin and components of the Myddosome in mammalian cells. *Proc*
421 *Natl Acad Sci U S A* **116**, 13293-13298, doi:10.1073/pnas.1905873116 (2019).
- 422 26 Otten, E. G. *et al.* Ubiquitylation of lipopolysaccharide by RNF213 during bacterial infection.
423 *Nature* **594**, 111-116, doi:10.1038/s41586-021-03566-4 (2021).
- 424 27 Ritorto, M. S. *et al.* Screening of DUB activity and specificity by MALDI-TOF mass spectrometry.
425 *Nat Commun* **5**, 4763, doi:10.1038/ncomms5763 (2014).
- 426 28 De Cesare, V. *et al.* Deubiquitinating enzyme amino acid profiling reveals a class of ubiquitin
427 esterases. *Proc Natl Acad Sci U S A* **118**, doi:10.1073/pnas.2006947118 (2021).

428

429

430

Figure 1

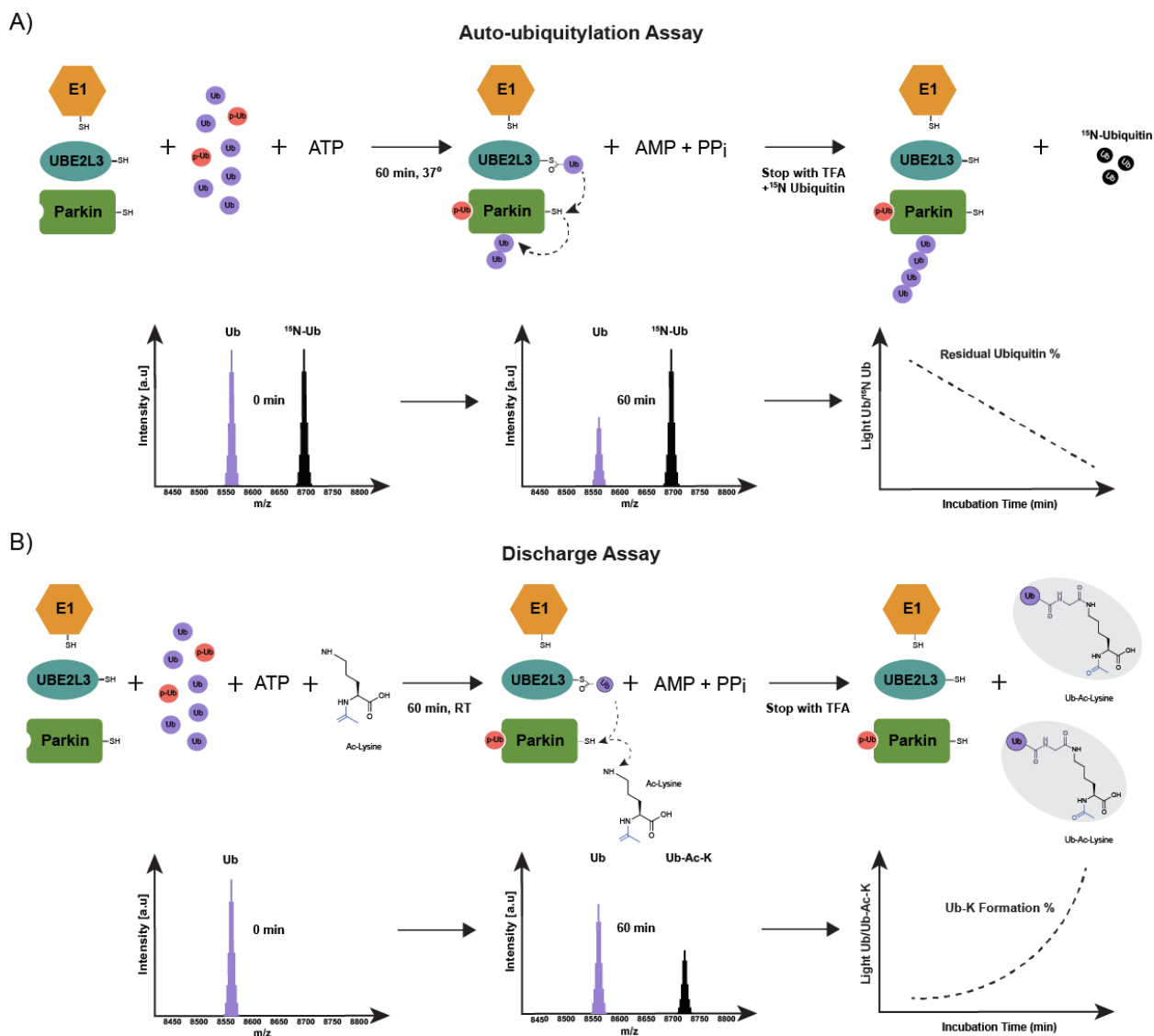
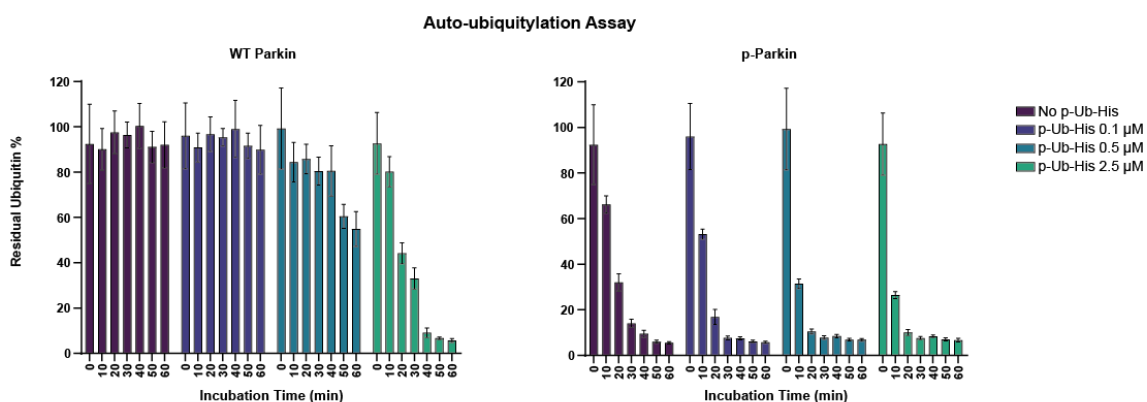


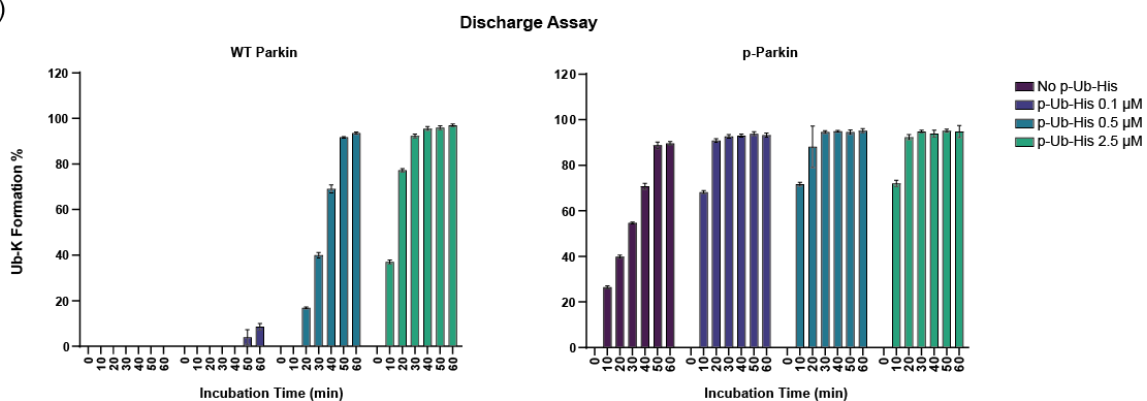
Figure 1 | Schematic representation of MALDI-TOF MS Parkin auto-ubiquitylation and discharge assay. A) Parkin auto-ubiquitylation reduces the pool of ubiquitin detected by MALDI-TOF MS over time. Quantification is achieved by use of ^{15}N ubiquitin as internal standard consistently present in the reaction (Light Ub/ ^{15}N Ub). B) Parkin-dependent formation of Ub-Ac-Lysine (Ub-K) is detected by MALDI-TOF MS. Quantification is achieved by measuring the ratio between the substrate (Ub) and the product (Ub-K). A linearity curve allows to translate Ub/Ub-K ratio into Ub-K formation %.

Figure 2

A)



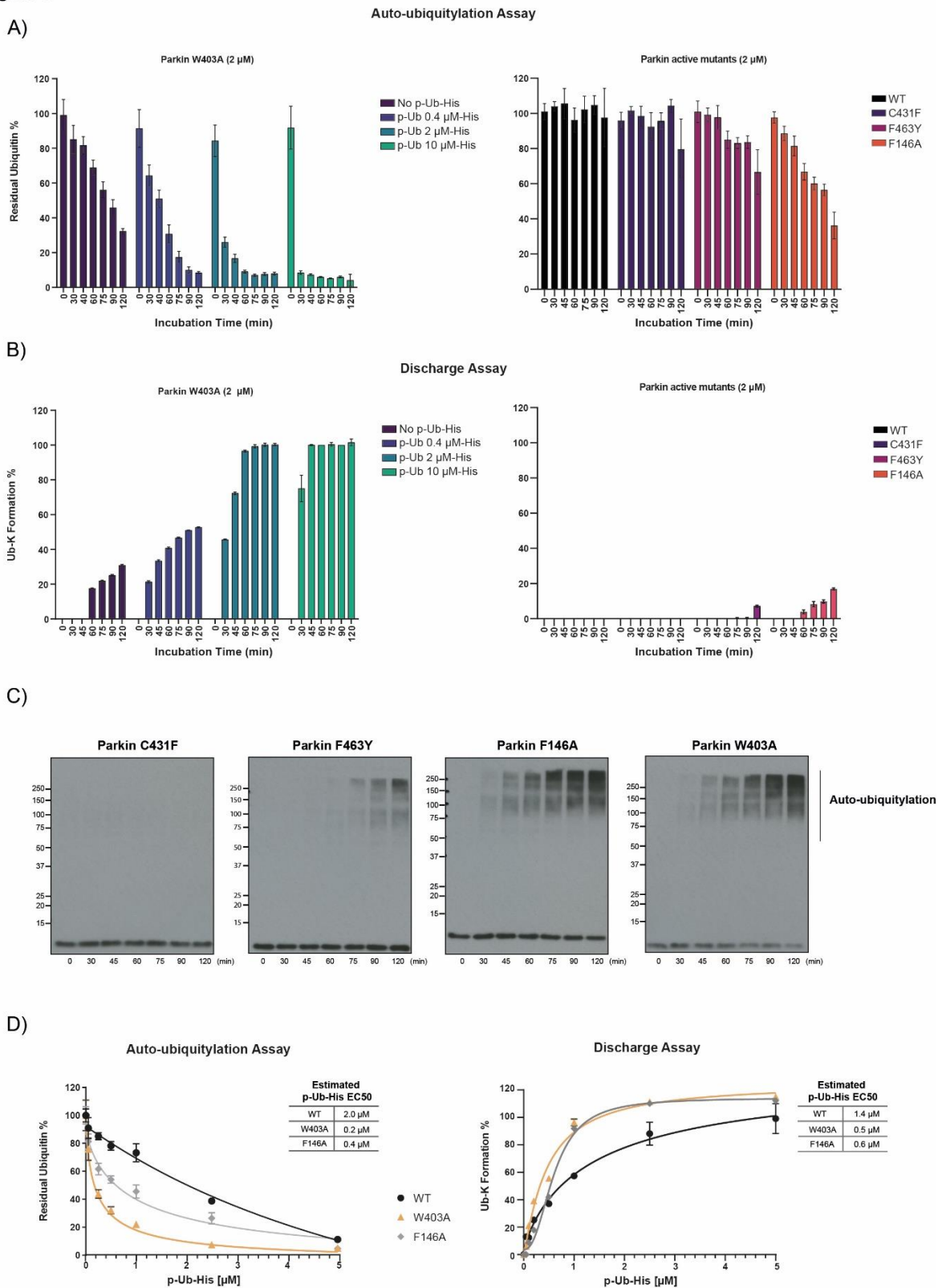
B)



439

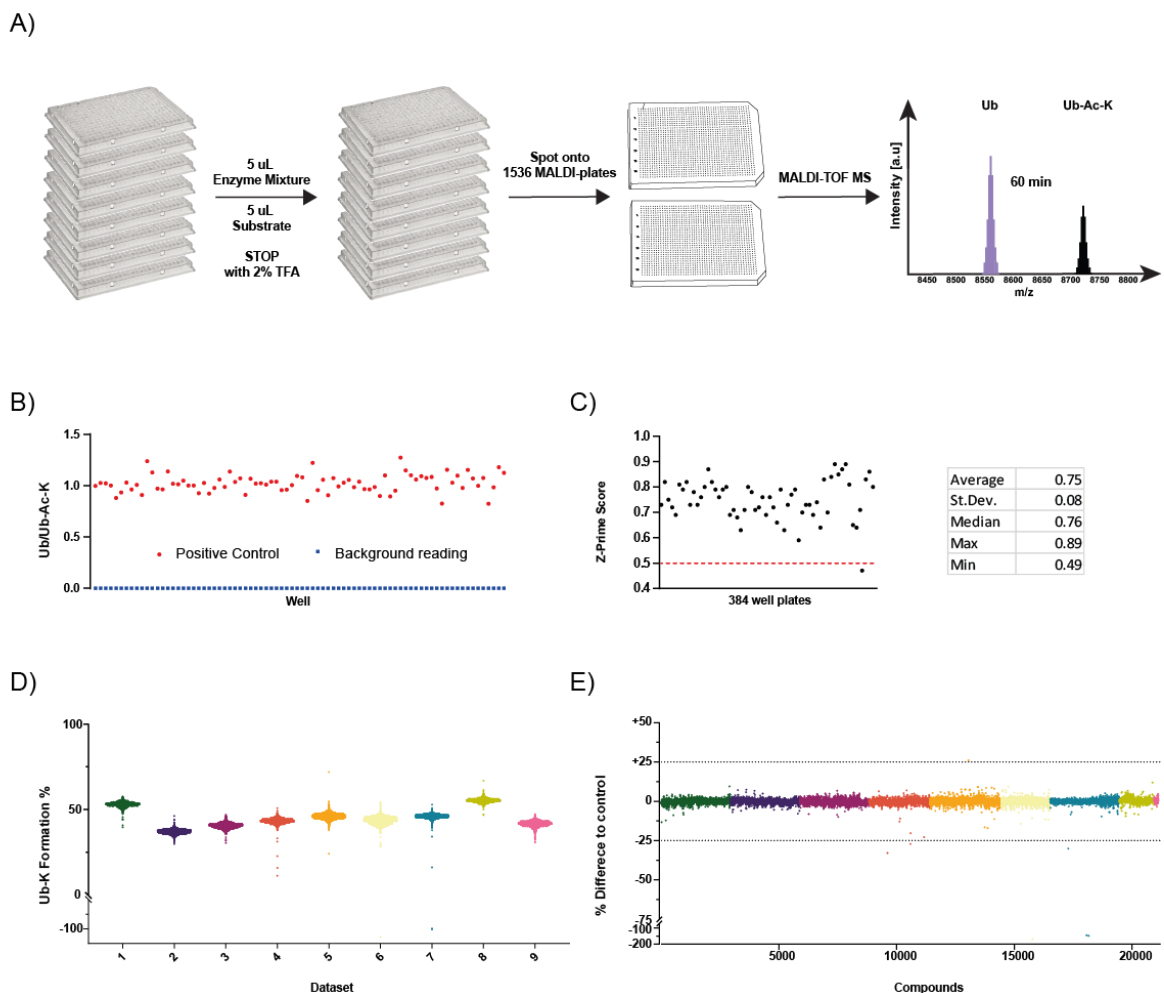
440 **Figure 2** Quantification of WT Parkin and p-Parkin activity by autoubiquitylation (A) and
441 discharge assay (B). WT Parkin and p-Parkin were incubated in absence or in presence of
442 increasing amount of p-Ub-His for up to 60 minutes. The reduction of mono-ubiquitin as
443 consequence WT Parkin and p-Parkin activity is reported as Residual Activity % (A) in
444 autoubiquitylation assay while the Ub-K % formation indicates activity in the discharge assay
445 read-out (B). Data points are reported as the average of 3 replicates \pm SD.

Figure 3



447 **Figure 3|** Quantification of Parkin mutants' activity by autoubiquitylation (A) and discharge
448 assay (B). All Parkin mutants were tested at 2000 nM final at the indicated time points. Results
449 were validated by Parkin *in vitro* ubiquitylation assay followed by SDS-page and western
450 blotting using anti-ubiquitin antibody (C). Estimated Half maximal effective concentration of p-
451 Ub-His for the activation of WT, W430A and F146A Parkin (D). Data points are reported as
452 the average of 3 replicates \pm SD

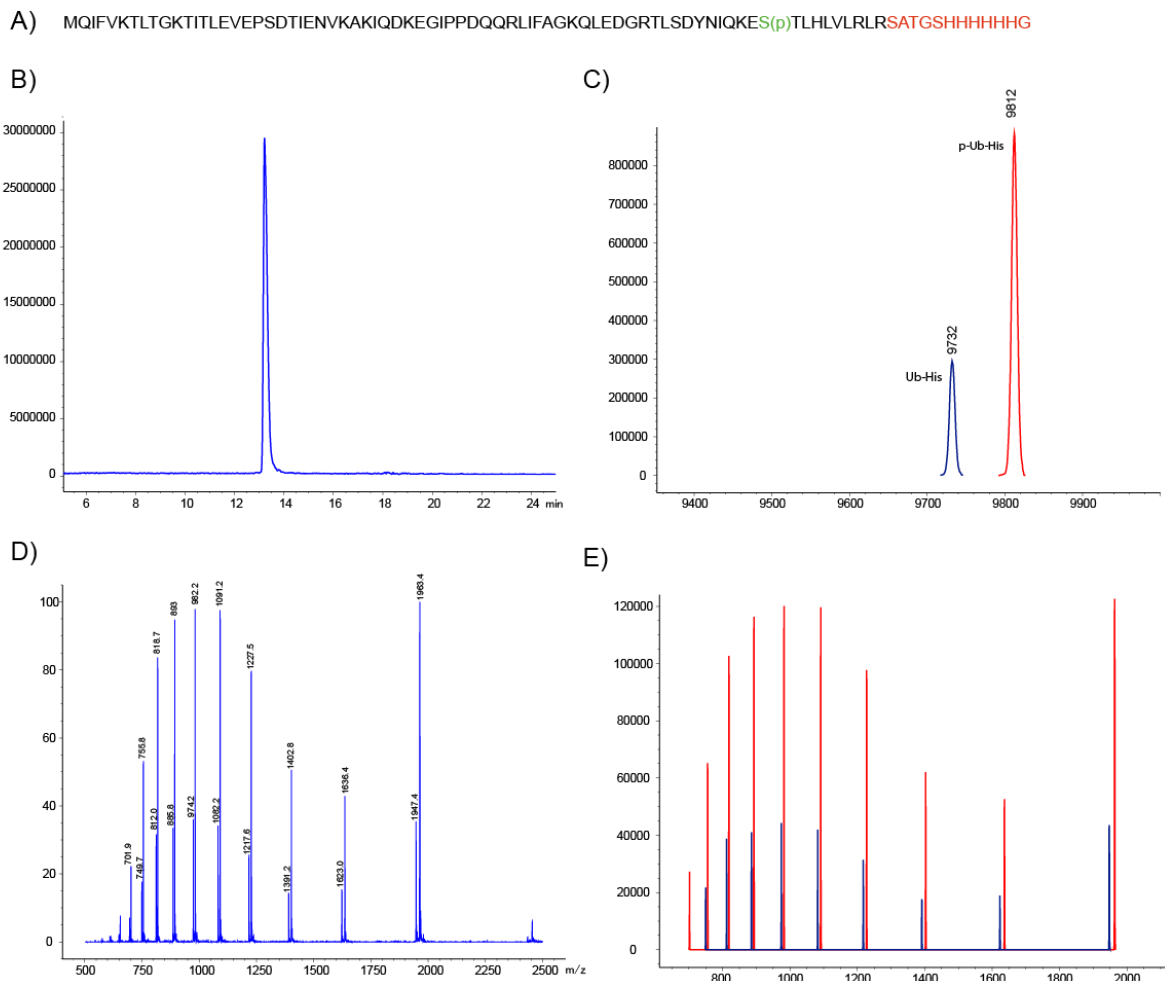
Figure 4



453 **Figure 4|** p-Parkin High-Throughput Screening by MALDI-TOF MS discharge assay.
454 Workflow schematic (A) and representative data of positive control and background reading
455 (B). Z' Prime value for HTS plates (C). Data distribution for independent datasets (experiments
456 were performed in single replicate) and compounded data of HTS normalized to the positive
457 controls for the identification of inhibitors and activators. Compounds have been tested as
458

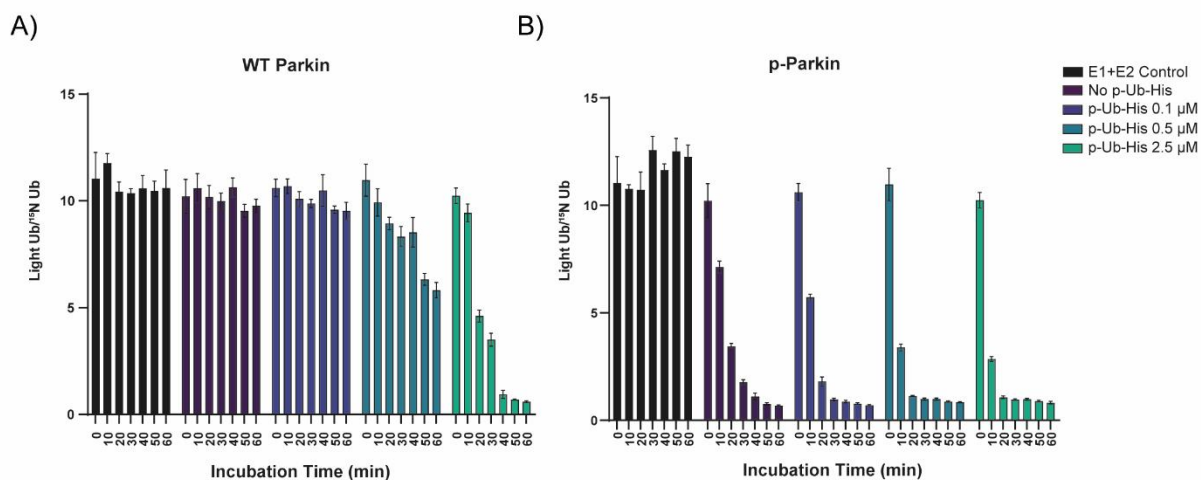
459 single replicates while 16 data points were included in each 384 well plate for both positive
460 and negative controls.

Sup. Figure 1

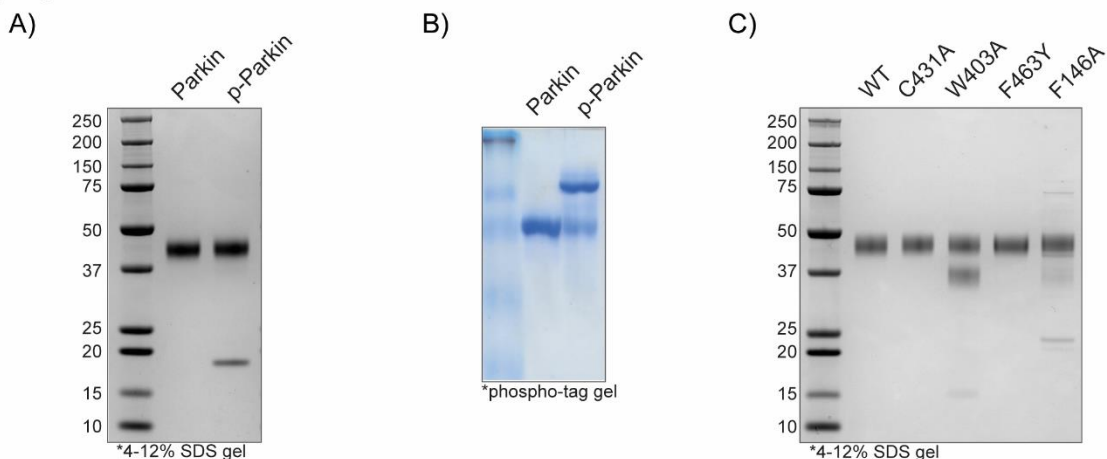


461

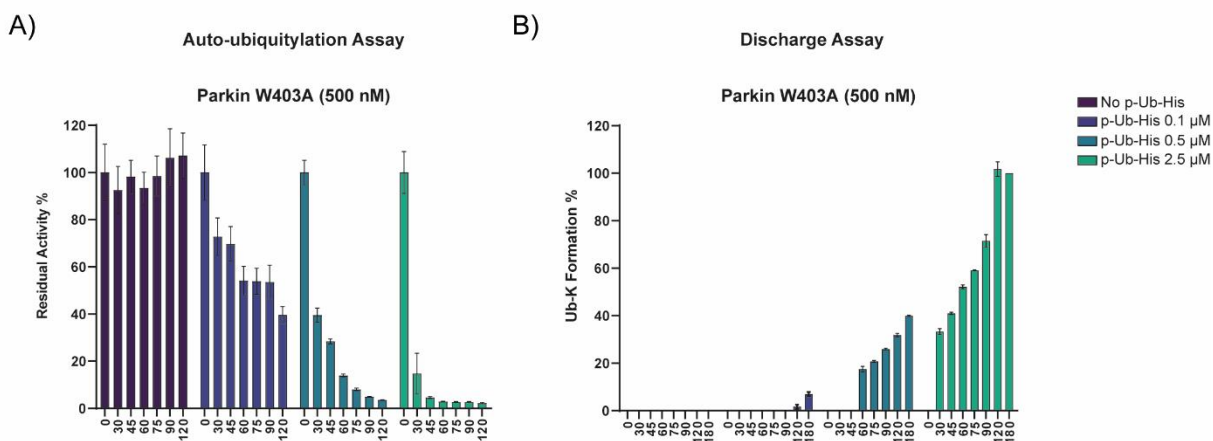
Sup Fig. 2



Sup Fig. 3



Sup Fig. 4

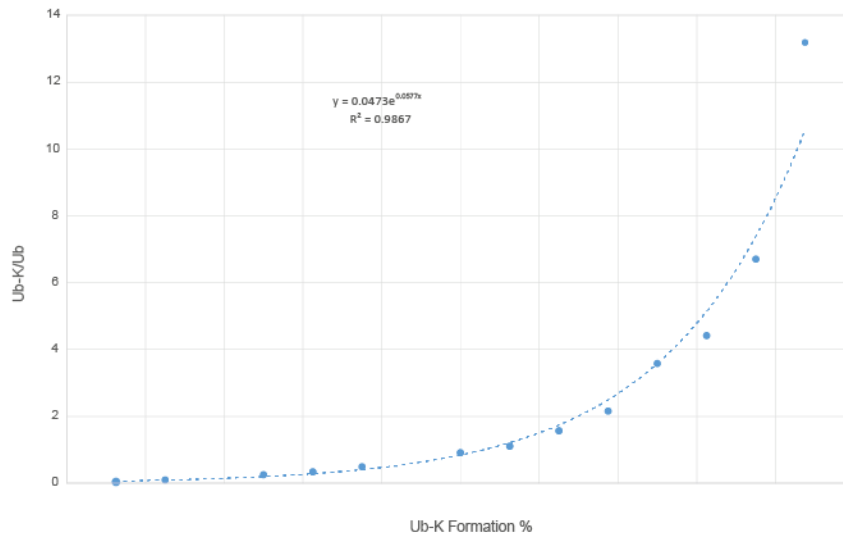


462

463

464

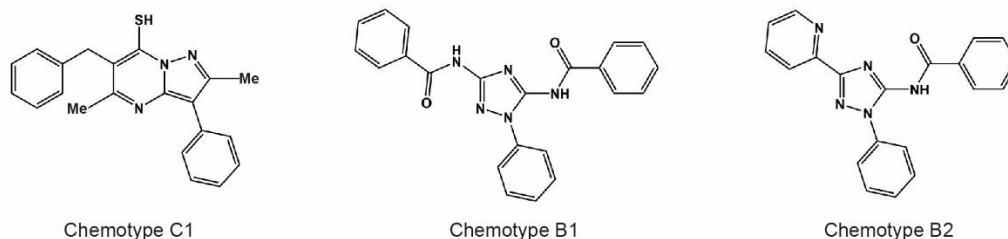
Sup Fig. 5



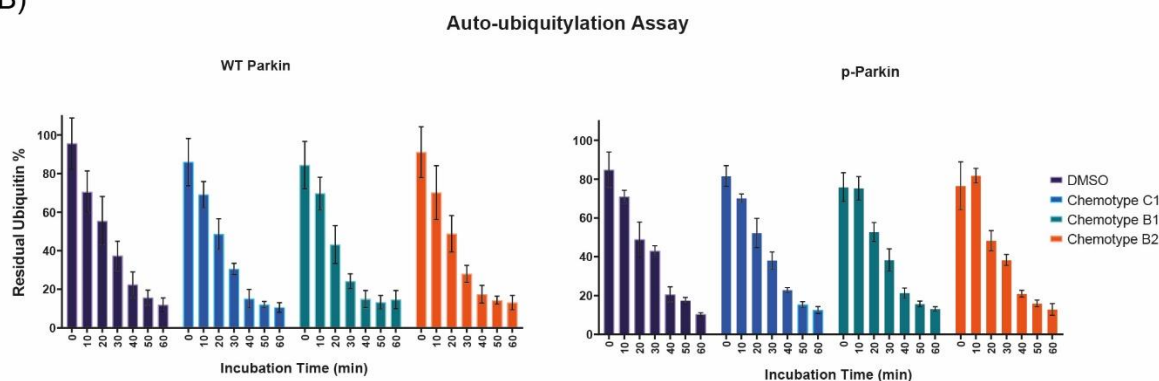
465

Sup Fig. 6

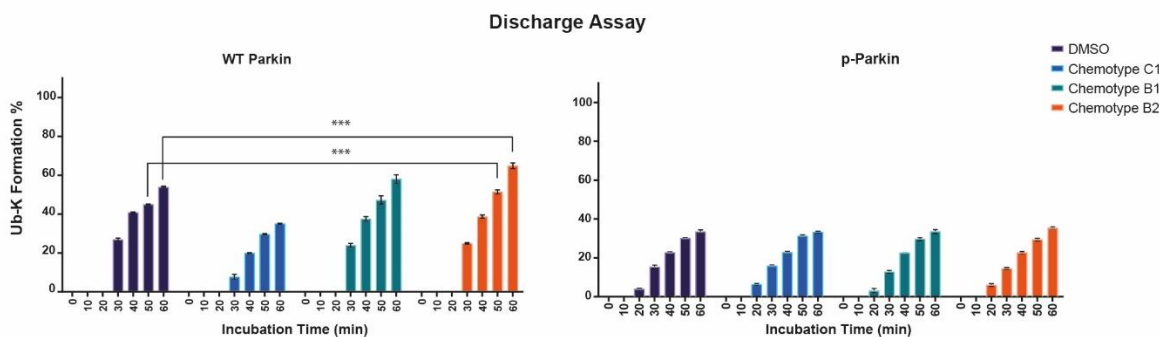
A)



B)



C)



466

467 **Sup Figure 1|His tagged Phosphorylated Ubiquitin (p-Ub-His) Quality Control.** p-Ub-His
 468 was expressed and purified as indicated in Methods. A) Protein sequence highlighted in green
 469 Serine 65 and in red 6His tag sequence. B) Chromatogram and C) MS components: 9812 m/z
 470 corresponding to the p-Ub-His expected m/z and 9732 m/z corresponding to the remaining
 471 not phosphorylated counterpart. Purity level have been considered into experimental
 472 calculations. D) Mass Spectrum and E) Deconvoluted Ion Set. p-Ub-His estimated at 70%.

473 **Sup. Figure 2| Light/¹⁵N ubiquitin ratio** before conversion into Remaining Ubiquitin %.
474 Stable level of light/¹⁵N ubiquitin in the E1+E2 control indicate no consumption of ubiquitin in
475 presence of the E1 activating enzyme and UBE2L3 conjugating enzyme only.

476 **Sup. Figure 3| Parkin, p-Parkin and activating Parkin mutants. A)** Parkin and p-Parkin
477 purity check by SDS-page. B) Parkin phosphorylation efficiency, phosphor-tag gels indicates
478 that p-Parkin is about 70% pure. C) Parkin activating mutants purity check by SDS-page.

479 **Sup. Figure 4| Parkin W403A autoubiquitylation (A) and discharge assay (B) at 500 nM.**
480 No background activity was detected when testing W403A at the final concentration of 500
481 nM.

482 **Sup. Figure 5| Linearity Curve for Ub-K formation %.** Known amount of Ub (substrate) and
483 Ub-K (product) were mixed and analysed by MALDI-TOF MS. Resulting curve and associated
484 exponential equation was employed to translate Ub-K/Ub peak area ratio into Ub-K
485 Formation%

486 **Sup. Fig. 6|** Evaluation of previously reported Parkin activators. Three compounds selected
487 from patent WO 2018/023029 (panel A: chemotype B1, B2 and C1) were tested against WT-
488 Parkin and p-Parkin at the final concentration of 50 μ M by autoubiquitylation (B) and
489 discharge assay (C). Reactions were stopped at the indicated time points. Data points are
490 reported as the average of 2 replicates spotted in duplicate (4 data points total) \pm SD.

491

492